

# **Numerical and experimental analysis of effort of human tooth hard tissues in terms of proper occlusal loadings**

GRZEGORZ MILEWSKI

Institute of Applied Mechanics, Cracow University of Technology,  
Al. Jana Pawła II 37, 31-864 Kraków, Poland, e-mail: milewski@mech.pk.edu.pl

The paper presents the results of strain gauge experiments conducted in order to determine the strain and stress distributions in all groups of human tooth crowns in terms of the proper occlusal loadings. The features simulating masticatory loadings have not been considered. The results have been compared with the numerical solutions obtained by means of finite element method (FEM). A good agreement between the results of both experiments has been reached. On that basis the analysis of effort distributions in enamel and dentine as well as comparison of application of strength hypotheses to hard tissues of tooth were made.

*Key words: strain gauge, FEM, effort, strength hypotheses, dentine, enamel*

## **1. Introduction**

Standards of occlusion for human teeth become individually differentiated, depending on the face shape, tooth location, shape of the alveolar arch and customized movements of mandible in physiological activities of biting and mastication (ŁASIŃSKI [6], KAHL-NIEKE [5]). Only a few types of occlusions, including the so-called edge-to-edge and end-to-end bites for anterior teeth and mutual occlusions by means of cusps for lateral teeth, are taken into account as proper. Strength tests and experimental model strain gauge analysis, presented in the paper, were carried out for all teeth groups, i.e. incisors, canines, premolars and molars, for occlusal loadings simulating the features of the above types of bites.

Although dentine and enamel seem to be very similar to the skeletal bone tissues, teeth are characterised by the endodermic genesis as, for instance, nails or hair. Compared to the bone structures, both compact and trabecular, hard tissues of teeth are highly mineralised. In the case of enamel, the rate of the mineral phase

reaches even more than ninety per cent. Such a structure of dentine and enamel, results in treating them also as highly isotropic materials (CURREY [3], CRAIG [1], CRAIG and PEYTON [2]). Table 1 presents a set of strength properties for hard tissues of tooth (after [4]).

As application of strength hypotheses in tooth structures is very rarely described in an available literature, the main aims of the combined experiments presented were as follows:

- comparison of the agreement of the results of both methods (experimental and numerical),
- analysis of the areas of tooth crowns that experience the greatest effort in terms of main rules of fillings applied in conservative dentistry,
- analysis of the application of strength hypotheses to dentine and enamel as highly isotropic materials.

Table 1. Strength properties of dentine and enamel [4]

Tooth structure	Dentine	Enamel
Modulus of elasticity $E$ [GPa]	18.6	84.1
Poisson's ratio	0.31	0.33
Tensile strength $\sigma_t$ [MPa]	105.5	10.3
Compressive strength $\sigma_c$ [MPa]	297	382
Tangential strength $\sigma_s$ [MPa]	138	90.2

## 2. Methods

The strain gauge tests were carried out for all tooth groups, i.e. incisors, canines, premolars and molars, with the use of INSTRON 4465 strength machine, multi-bridge strain gauge UPM 40 A set and DMClab Hottinger unit for data acquisition (figure 1). All characteristic surfaces of every tooth, i.e. mesial, distal, buccal and lingual surfaces whose strain rosettes were cemented, were analysed.

On the other hand, the numerical analysis of strain and stress fields in the loaded tooth crowns is made by means of finite element method (FEM) with ANSYS<sup>®</sup> software.

The effort in tooth dentine and enamel was analysed by means of the following strength hypotheses used for isotropic materials: von Mises ( $\sigma_M$  – equation (1)), Tresca–Guest ( $\sigma_{T-G}$  – equation (2)), de Saint-Venant ( $\sigma_{S-V}$  – equation (3)) and Burzyński–Torre ( $\sigma_{B-T}$  – equation (4)). The last theory is considered to be the best and the most effective hypothesis for both ductile and brittle materials (ŻYCZKOWSKI [8]).

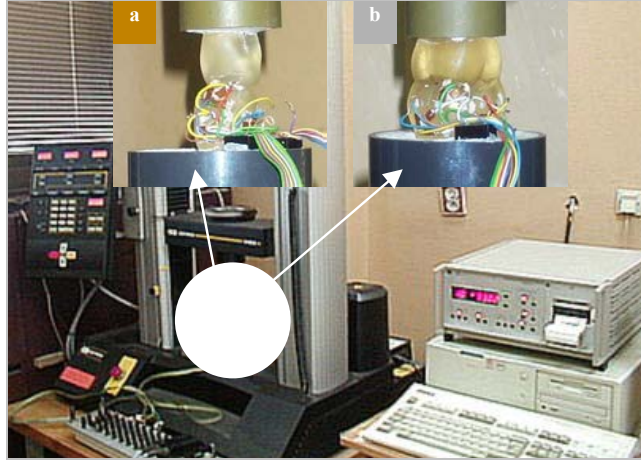


Fig. 1. Strain gauge experiment for anterior (a) and lateral (b) tooth occlusions

The relevant equations for the reduced stress  $\sigma_{\text{red}}$  according to the above hypotheses are as follows:

- The von Mises reduced stress

$$\sigma_{\text{red}} = \sigma_M = \sigma_e = \sqrt{\frac{3}{2} s_{ij} s_{ij}} = \frac{1}{\sqrt{2}} \sqrt{(\sigma_1 - \sigma_2)^2 + (\sigma_2 - \sigma_3)^2 + (\sigma_3 - \sigma_1)^2}, \quad (1)$$

where  $s_{ij}$  denotes deviatoric stress and  $\sigma_m$  stands for mean stress

$$s_{ij} = \sigma_{ij} - \delta_{ij} \sigma_m, \quad \sigma_m = \frac{1}{3} \sigma_{kk}. \quad (1a)$$

- The Tresca–Guest hypothesis

$$\sigma_{\text{red}} = \sigma_{T-G} = \sigma_1 - \sigma_3. \quad (2)$$

- The de Saint-Venant strength hypothesis ( $\epsilon_{\text{max}}$ )

$$\sigma_{\text{red}} = \sigma_1 - \nu(\sigma_2 + \sigma_3). \quad (3)$$

- The Burzyński–Torre reduced stress

$$\sigma_{\text{red}} = \sigma_{B-T} = \frac{1}{2\kappa_c} \left\{ 3(\kappa_c - 1)\sigma_m + \sqrt{\left[ 9(\kappa_c + 1)^2 - 12 \frac{\kappa_c^2}{\kappa_s^2} \right] \sigma_m^2 + \frac{4\kappa_c^2}{3\kappa_s^2} \sigma_e^2} \right\}, \quad (4)$$

where

$$\kappa_c = \frac{\sigma_c}{\sigma_r}, \quad \kappa_s = \frac{\sigma_s}{\sigma_r}, \quad \sigma_e = \sqrt{\frac{3}{2} s_{ij} s_{ij}}. \quad (4a)$$

### 3. Results

Experimental model strain gauge analyses were carried out for sequential loading and unloading paths in range of 5–200 N, depending on the kind of tooth. The tests were conducted on epoxy resin tooth models in scale 5:1. In the calculations of the strain and stress values for the real tooth structure (enamel), the conditions of the model similarity concerning Young's modulus and Poisson's ratio were accepted, i.e.  $E_{\text{enamel}}/E_{\text{epoxy}} = 30$  and  $\nu_{\text{enamel}} = \nu_{\text{epoxy}}$ . The above values of loads provided elastic strains and practically linear hysteresis loops for each kind of tooth. Figure 2 presents, for instance, the distributions of the principal stresses  $\sigma_1$  and  $\sigma_2$  in the enamel of canine after calculations with regard to the model similarities and scale effect.

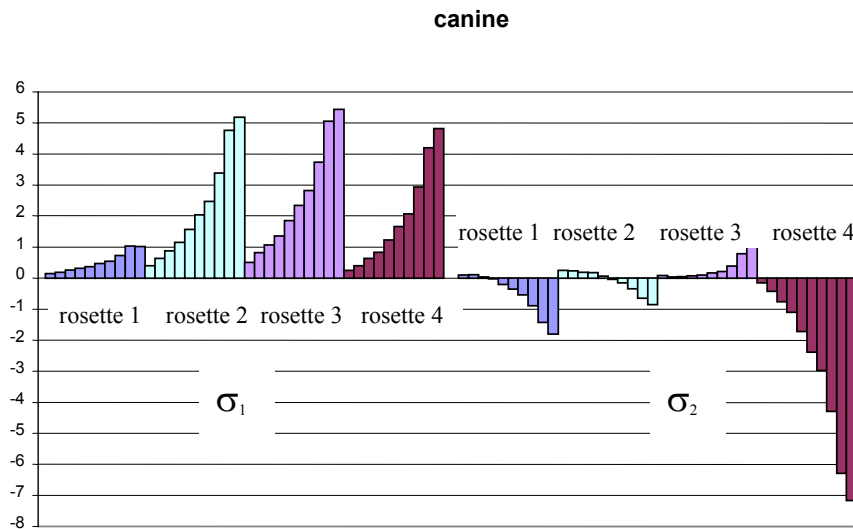


Fig. 2. Principal stresses  $\sigma_1$  and  $\sigma_2$  [MPa] in canine crown for loading path

The results of strain gauge experiments show that the greatest effort areas of teeth lie at the base of crowns up to the gingival line. That regularity exists for incisors, canines and premolars. Only in the case of molars, the areas close to the cusps are characterized by higher values of stresses. The highest stresses at incisor base crown are exerted on lingual and buccal surfaces. For lingual surface the maximal values of stresses at tooth loading of 200 N reach 15 MPa. In the case of canine, lingual surface at crown base experiences the greatest effort. At loading of 110 N the maximum stresses exceed 7 MPa, while on buccal side they reached 5 MPa. Also mesial and distal surfaces seem to experience quite strongly the effort (the stress higher than 5 MPa). In case of incisor, those surfaces experience the effort that is 2–3 times less compared with that on the lingual side. All characteristic surfaces of molars and premolars are characterized by relatively equal effort. The maximum principal stress

values at crown base approached 4 MPa for molars and premolars at 70 N for 100 N, respectively. In the case of molars, the areas of crown cusps that experience the greatest effort produce maximal stresses exceeding 16 MPa. For premolars, whose cusps are less shaped, the relevant stress values approach 2 MPa.

A comparison of the effort of each tooth group seems to be very interesting. Figure 3 illustrates the values of maximum principal stresses  $\sigma_1$  and  $\sigma_2$  at the same loading of 70 N for each teeth. The tooth that experience the greatest effort can be arranged according to the following order: molars, canines, incisors and premolars. This corresponds quite well to the clinical observation.

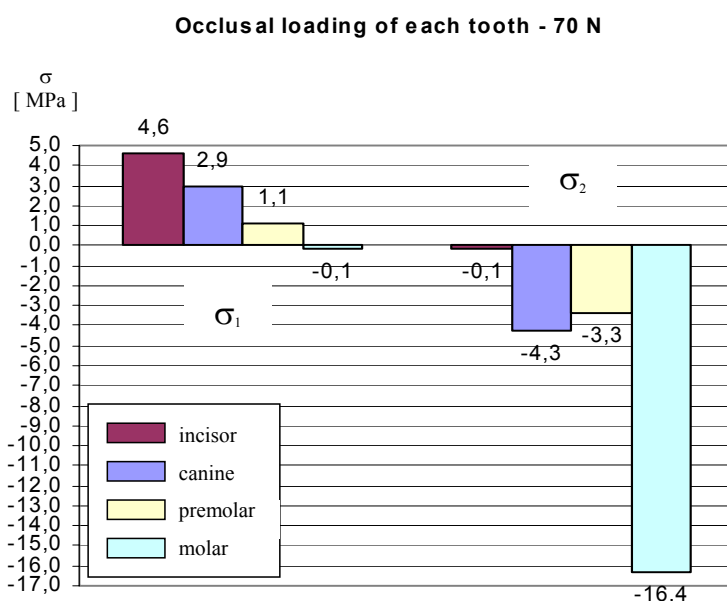


Fig. 3. Comparison of the maximum values of the principal stresses  $\sigma_1$  and  $\sigma_2$  in tooth enamel at occlusal loading of 70 N for each tooth group

Numerical analyses of the stress and strain fields in tooth crowns were carried out by means of finite element method. In order to compare the results of both, i.e. those of strain gauge and numerical experiments, canine tooth was chosen. Geometry of a tooth was exactly the same, as a configuration of the outer geometry of canine model was obtained by means of 3-D scanning procedure using Leitz PMM 12106 equipment. Then with the use of Mechanical Desktop<sup>®</sup> and FEMAP<sup>®</sup> programs the other structures of tooth were modeled (MILEWSKI [7]).

Figure 4 presents, for instance, the distributions of the values of principal strains  $\varepsilon_1$ ,  $\varepsilon_2$  on the relevant four surfaces of canine crown. On the other hand, table 2 gives the comparison of the above quantities in strain gauge experiment and numerical calculations for canine at the occlusal loading of 50 N. Settlements of strain rosettes on

tooth crown are as follows: 1 – buccal surface at top crown edge, 2 – distal surface at crown base, 3 – buccal surface at crown base, 4 – lingual surface at canine crown base.

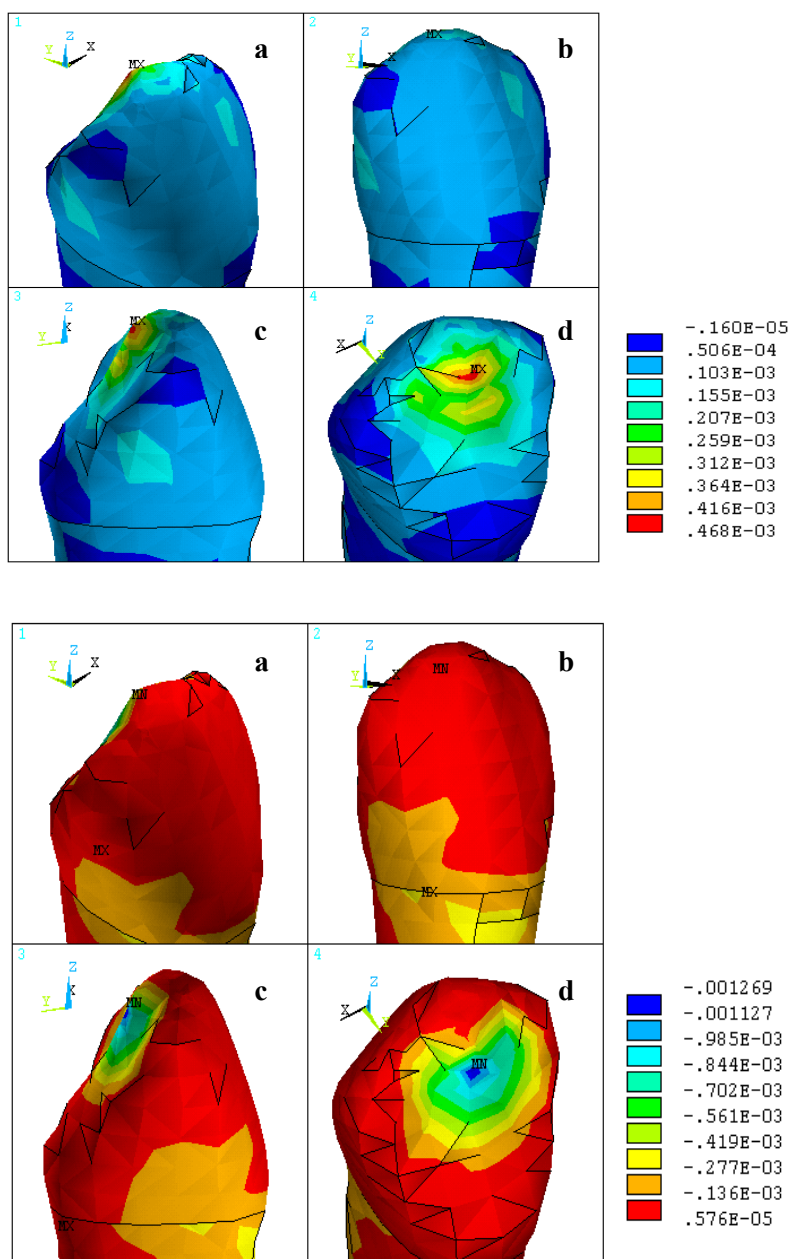


Fig. 4. Distributions of the principal strains  $\varepsilon_1$  and  $\varepsilon_2$  on the relevant four characteristic surfaces of canine crown at a proper occlusal loading of 50 N

Table 2. Comparison of principal strain values  $\varepsilon_1$ ,  $\varepsilon_2$  and von Mises equivalent stress  $\sigma_M$  in strain gauge experiment and numerical calculations for canine at occlusal loading of 50 N

Tooth crown area	$\varepsilon_1 [\times 10^{-6}]$		$\varepsilon_2 [\times 10^{-6}]$		$\sigma_M [\text{MPa}]$	
	Strain gauge	FEM	Strain gauge	FEM	Strain gauge	FEM
1	44	68	-43	-47	0.92	1.24
2	150	96	-57	-113	2.53	2.92
3	215	124	-95	-116	2.72	2.81
4	181	131	-217	-179	4.36	4.71

Agreement of the results of both experiments seems to be quite satisfactory; for stresses the medium error is 12%, while for strains it reaches 22%. Analysis of the results points out that the areas of tooth crowns that experience the greatest effort lie at the base of the crowns, close to the gingival line. That regularity is observed for incisors, canines and premolars. Only in the case of molars, the maximum stress is measured in the areas of tooth cusps. It is worth stressing that no mastication areas were examined in strain gauge test due to the limitation of the method, mainly concerning the placement of the rosettes that are close to the occlusal tooth contact areas.

The other aim of the paper was to analyze the possibilities of applying the well-known strength hypotheses accepted for hard tissues of tooth, i.e. dentine and enamel. The detailed stress and strain analyses were done in the areas of the incisor crown structures being characterized by the maximum effort, i.e. occlusal contact zone in the enamel, gingival line areas, both in the dentine and enamel, dentine regions close to the pulp chamber (figure 5).

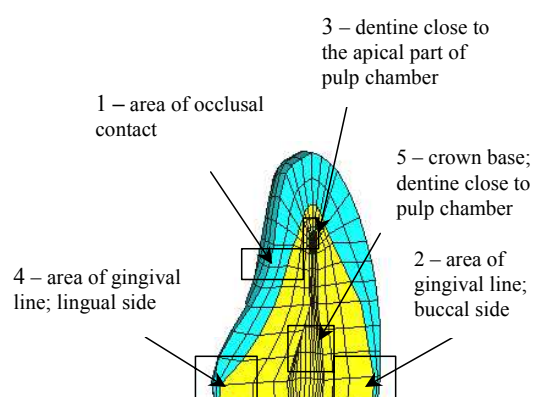


Fig. 5. Characteristic areas of the incisor crown where the strength hypotheses were compared

A comparison of the maximum values of effort in the incisor dentine and enamel for the strength hypotheses under consideration was done with the reference to the variable occlusion angle  $\varphi$ , whose value in the numerical simulation was equal to  $0^\circ$ ,

20°, 25°, 30°, 45° and 90°. Null angle represents the so-called edge-to-edge bite, the angles equal to 20°, 25° and 30° represent typical proper occlusions for human incisors, and the angles of 45° and 90° denote, respectively, pathological and hypothetical occlusions.

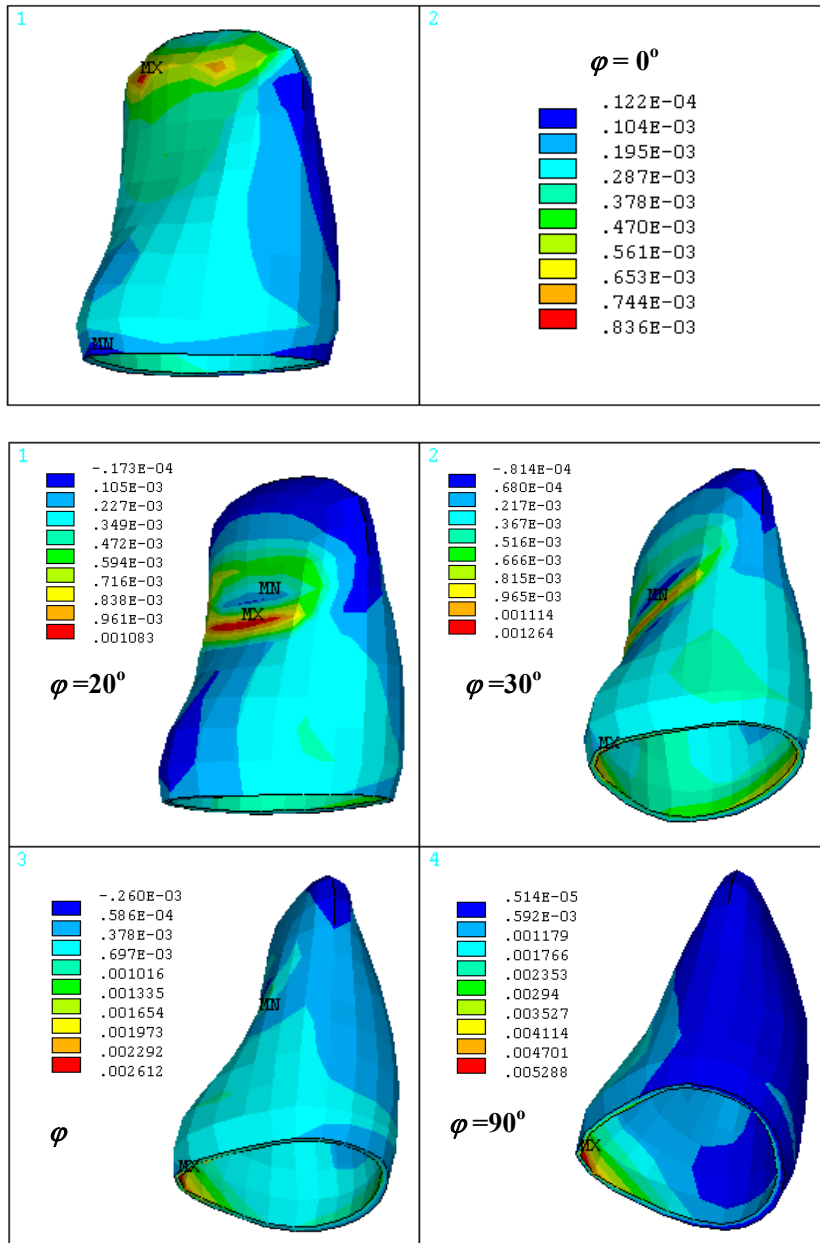




Fig. 6. Distribution of the maximum principal strain  $\varepsilon_1$  in the incisor enamel at various occlusal angles

The examples of the maximum principal strain  $\varepsilon_1$  distributions (de Saint-Venant) in the incisor enamel are given in figure 6, while the von Mises reduced stress distributions are presented in figure 7. In both cases, the value of the occlusal loadings was 500 N.

The maximum values of effort in the incisor dentine and enamel obtained based on the strength hypotheses under consideration are compared in table 3. The comparison was done with the reference to the variable occlusion angle  $\varphi$  in the characteristic areas of effort: occlusal contact zone (A), base of a tooth crown near the gingival line: lingual site (B), buccal site (C), dentine close to the apical region of pulp chamber (D).

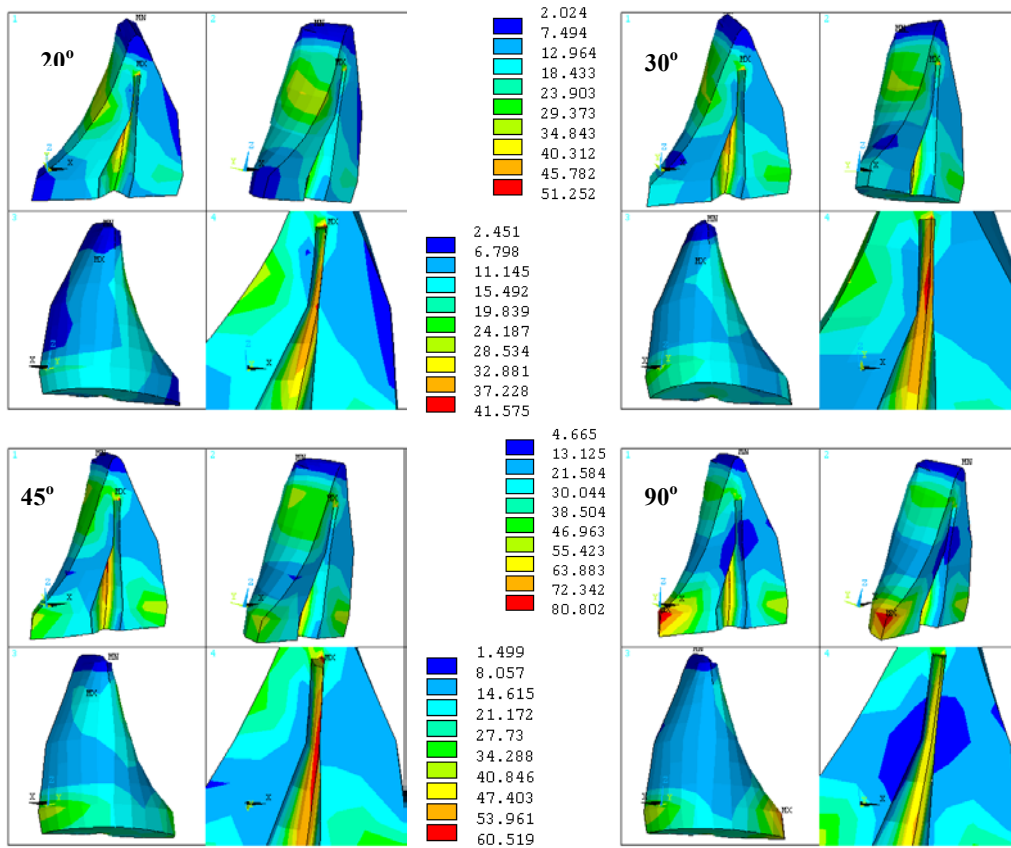


Fig. 7. Distributions of the von Mises reduced stress  $\sigma_M$  [MPa] in the incisor dentine at various occlusal angles

The results of the numerical analysis of effort in the hard tissues of anterior teeth were compared with the experimental strength tests carried out on extracted teeth. Figure 8 shows two typical kinds of crown fractures in anterior teeth for various ways of occlusal loadings. The first case, an oblique fracture line, is characteristic of a proper occlusions (at  $\varphi$  up to  $30^\circ$ ), while the second one, fracture of crown base, appears more often at higher values of occlusal angle  $\varphi$ , where bending effects dominate.

Table 3. Comparison of the maximum values of effort in the incisor dentine and enamel for various strength hypotheses

$\varphi$ [°]	Area	Tooth structure	$\sigma_M$ [MPa]	$\sigma_{T-G}$ [MPa]	$\sigma_{B-T}$ [MPa]	$\varepsilon_1 [\times 10^{-4}]$
0	A	Enamel	160.0	174.3	7.2	8.4
	B	Dentine	15.5	15.9	5.5	3.6
20	A	Enamel	168.2	192.2	5.7	10.8
	D	Dentine	41.6	45.2	16.7	8.3
25	A	Enamel	158.8	182.5	5.2	10.8
	D	Dentine	47.6	52.0	19.2	9.9
30	A	Enamel	149.8	172.7	4.8	12.6
	D	Dentine	51.2	56.2	20.6	10.9
45	B	Enamel	224.1	256.4	313.6	26.1
	D	Dentine	60.5	66.9	24.2	18.0(B)
90	B	Enamel	450.9	514.0	624.6	52.9
	B	Dentine	80.8	86.9	45.5	30.3

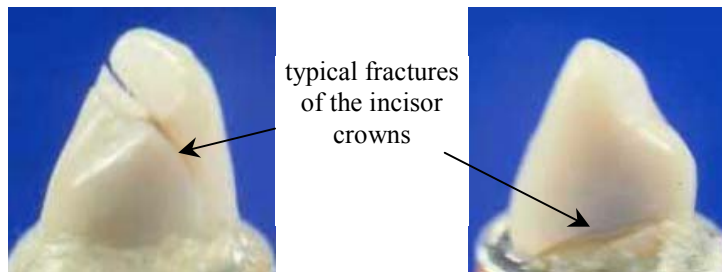


Fig. 8. Characteristic fractures of anterior tooth crowns at various occlusal loadings

For the lateral teeth (premolars and molars) a comparison of the considered strength hypotheses is presented in table 4. With the reference to the described earlier localizations of the effort areas (A–D), an additional area E represents the dentine zones in the upper part of the crown, close to the mastication surface.

The example of the reduced von Mises stresses ( $\sigma_M$ ) distribution in the premolar crown at a normal occlusion of 500 N is presented in figure 9 for the mesial-distal cross section (a) and for the enamel part only (b).

Table 4. Comparison of the strength hypotheses for the maximum effort in premolar dentine and enamel for proper occlusion of 500 N

Area	Tooth structure	$\sigma_M$ [MPa]	$\sigma_{T-G}$ [MPa]	$\sigma_{B-T}$ [MPa]	$\varepsilon_1 [\times 10^{-4}]$
A	Enamel	45.9	48.1	1.4	2.0
B	Enamel	25.3	25.9	0.6	1.1
E	Dentine	16.8	17.7	5.9	3.5
D	Dentine	16.6	18.3	6.1	3.9
B	Dentine	15.9	16.7	9.3	1.4

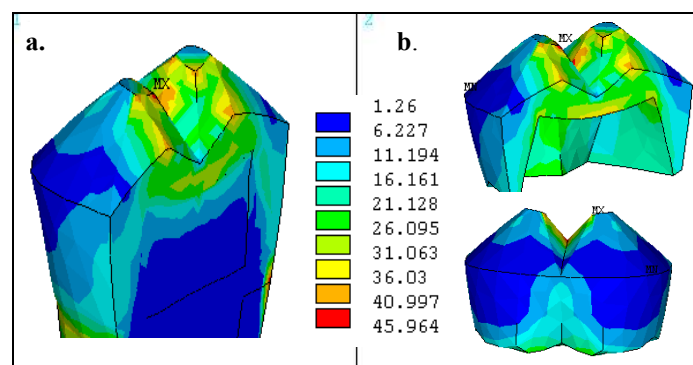


Fig. 9. Distribution of the reduced von Mises stresses  $\sigma_M$  [MPa] in premolar crown at normal occlusion of 500 N

On the other hand, the examples of the accompanying strength tests carried out on the extracted lateral teeth are shown in figure 10. The destructions of tooth crowns characteristic of the normal occlusions (figure 10a) and of the masticatory movements (destructions of the separate cusps, figure 10b) were in a majority.

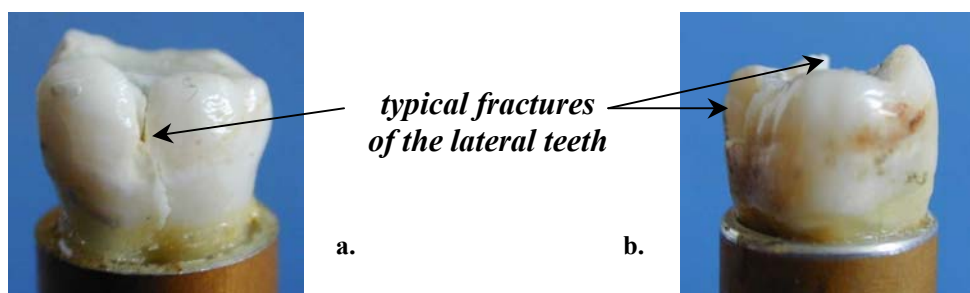


Fig. 10. Characteristic fractures of lateral tooth crowns under various occlusal loadings

#### 4. Conclusions

A combined approach to application of experimental stress analysis method and numerical FEM simulations enables a reliable assessment and estimation of the effort of hard tooth tissues in terms of occlusal loadings. Consistence of the results obtained renders possible a proper application of numerical models as less time-consuming and more effective pre-clinical tests concerning the strength aspects of tooth occlusion and fillings techniques in contemporary conservative dentistry.

Numerical simulations and experimental strength tests prove that, especially for dentine, the areas of maximum effort correspond to the distributions of the maximum tangential stresses. This implies the correctness of applying both the von Mises and Tresca–Guest strength hypotheses. The appearance of cracks in the enamel in the occlusal contact zone as well as in the area of the crown base testifies to the usefulness of the hypothesis of the maximum principal strain  $\varepsilon_1$ . It is also worth stressing a relatively wide spread of the effort estimation according to the Burzyński–Torre hypothesis, both in the dentine and enamel. As the result of the great negative values of the I invariant of the stress tensor (mean value) for the proper occlusal loadings the reduced stress values  $\sigma_{B-T}$  are relatively low compared with  $\sigma_M$  and  $\sigma_{T-G}$  values. For the cases of strong bending effects for anterior teeth and for mastication loadings in lateral teeth the respective values of  $\sigma_{B-T}$  rapidly increase. Those effects also seem to be a result of the strong asymmetry of dentine, and especially enamel, at tension, compression and shearing.

#### References

- [1] CRAIG R.G. (editor), *Restorative Dental Materials*, 9<sup>th</sup> ed., C.V. Mosby, Saint Louis, 1993.
- [2] CRAIG R.G., PEYTON F.A., *Elastic and mechanical properties of human dentine*, J. Dent. Research, 1958, Vol. 37, No. 4, pp. 661–668.
- [3] CURREY J.D. et al., *Bone Cell and Tissue Mechanics*, C.I.S.M., Udine, 1995.

- [4] [http://www.lib.umich.edu/libhome/Dentistry.lib/Dental\\_tables](http://www.lib.umich.edu/libhome/Dentistry.lib/Dental_tables).
- [5] KAHL-NIEKE B., *Introduction to orthodontia* (in Polish), Urban & Partner, Wrocław, 1999.
- [6] ŁASIŃSKI W., *Head anatomy for dentists* (in Polish), PZWL, Warszawa, 1978.
- [7] MILEWSKI G., *Strength aspects of biomechanical interaction bone tissue-implant in dental biomechanics* (in Polish), Assistant Prof. Thesis, Kraków, 2002.
- [8] ŻYCZKOWSKI M., *Discontinuous bifurcation in the case of the Burzyński-Torre yield condition*, Acta Mechanica, 1999, Vol. 132, pp. 19–35.